

**Introduction:** The imagery acquired by the Narrow Angle Camera (NAC) of NASA’s Lunar Reconnaissance Orbiter Camera (LROC) is a valuable dataset for lunar topographic mapping because of its very high resolution of 0.5-2 m/pixel. The NAC has a unique configuration consisting of two separate cameras (NACL and NACR) closely mounted. This configuration enables the collection of lunar surface images with both large coverage and high resolution. However, the mapping results from the NAC images depend highly on the accuracy of the relative alignment (referred to as boresight offset) between the two cameras. We present a boresight calibration approach for NAC imagery to remove the mapping inconsistencies due to the incorrect boresight offsets. Its performance is compared with the results derived from the standard SPICE kernels and the temperature-dependent SPICE kernels newly released by the LROC team [1].

**Relative Orientation between NACL and NACR:** The relative orientation between the NACL and NACR is denoted by boresight offsets including three translation offsets and three rotation angles. The translation offsets describe the positional offsets between the two cameras linearly. The rotation angles define the angular difference in the pointing directions of the cameras. These six parameters are defined in the LRO spacecraft frame and can be retrieved from the SPICE kernels. Among the six parameters, only the three angular parameters need to be calibrated because the error caused by angular parameters is proportional to the orbit height, while the influences of the possible errors in the translational boresight parameters are negligible and unlikely to be variable on a detectable level.

Figure 1 illustrates the three angular boresight offsets.  $\omega_b$  is the rotation angle of the boresight of NACL with respect to that of NACR around the X-axis (flight direction) in the NAC camera frame.  $\phi_b$  is the rotation angle of the boresight of NACR with respect to that of NACL around the Y-axis.  $\kappa_b$  is the rotation angle of the boresight of NACL with respect to that of NACR around the Z-axis (nadir) [2].

We examine two versions of the SPICE kernels of the LRO NAC imagery. One is the standard version generated by the LRO Mission Operations Center (MOC) retrieved from NAIF website and the other is an improved version of temperature-dependent SPICE kernels recently released by the LROC team [1]. The temperature-dependent SPICE kernels contain an updated frames kernel, an updated instrument kernel, and a series of new C-matrix kernels. They provide im-

proved orientation parameters for NAC imagery, which are temperature dependent [1]. The angular boresight offsets are therefore also temperature-dependent and varying for different NAC images. The temperature-dependent SPICE kernels are included in the data files of the current version of the USGS ISIS 3 package, and we retrieve the improved orientation parameters for NAC imagery from them in ISIS 3.

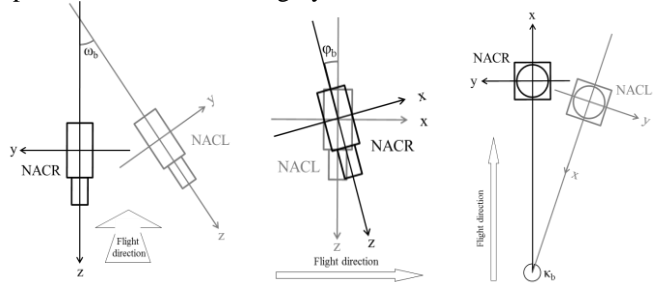


**Figure 1:** Conceptual illustration of the angular boresight offsets: omega  $\omega_b$  (left), phi  $\phi_b$  (middle), and kappa  $\kappa_b$  (right).

**Boresight Calibration of NAC Imagery:** The approach herein uses tie points obtained from the stereo images for the calibration. The tie points should be triple or quadruple matching points between the four images of a stereo pair. From the image orientation parameters, two sets of 3D coordinates of the tie points can be obtained from different stereo configurations of the NAC images. Ideally, these two sets of 3D coordinates should be consistent because they represent the same surface features. However, this is not the case due to the possible errors in the boresight offsets. These errors or inconsistencies can be reduced through a least-squares adjustment based on the geometric model of the NAC stereo images [3]. The observations of the adjustment include the tie points, the 3D ground coordinates of the tie points, the boresight parameters, and the image orientation parameters. Different weights are assigned to different observations. The outputs of the adjustment are the calibrated boresight offsets and improved image orientation parameters, from which lunar topographic models with improved consistency and precision can be generated.

**Experiments using NAC Images at the Apollo 15 Landing Site:** A NAC stereo pair covering the Apollo 15 landing site was employed for experimental analysis. The spatial resolutions of the images are 0.5 m/pixel. The image orientation parameters derived from the standard SPICE kernels are used to generate a DEM with a resolution of 1.5 m as shown in Figure 2

(a). It can be noticed that there are obvious differences in elevation (about 70 m) along the midline. This is mainly due to the inaccurate boresight parameters existing in the standard SPICE kernels. The image orientation parameters derived from the temperature-dependent SPICE kernels are also used to generate a DEM with the same resolution as shown in Figure 2 (b). It can be seen that the differences in elevation have been relieved, which proves the improvement of the temperature-dependent SPICE kernels to the boresight parameters. However, there are still small discrepancies (5-10 m) exist in the generated DEM. The proposed method is used to calibrate the angular boresight offsets of the image set. From the calibrated boresight offsets, improved image orientation parameters are obtained and they are used to generate a DEM with the same resolution as shown in Figure 2 (c). It can be seen that the differences in elevation are gone and the terrain surface is smooth.

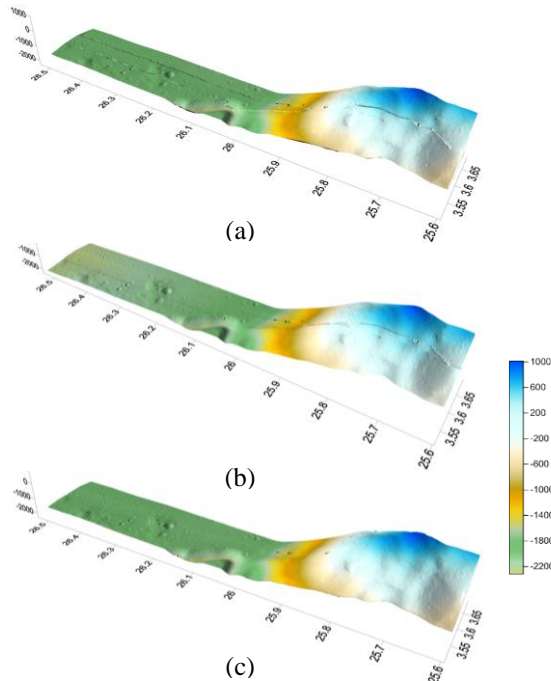


**Figure 2:** DEMs generated from NAC images at Apollo 15 landing site: (a) using the standard SPICE kernels, (b) using the temperature-dependent SPICE kernels, and (c) after boresight calibration.

Figure 3 provides a straightforward comparison of the orthorectified NACL and NACR image pairs generated using different ways. Figure 3 (a) is the orthorectified image pair generated in ISIS 3 using the temperature-dependent SPICE kernels. The Apollo 15 landing area is marked on the image using a rectangle. Figure 3 (b) is a close-up view of the area in the orthorectified image pair generated using the standard

SPICE kernels. Obvious offsets between the orthorectified image pairs can be seen. Figure 3 (c) is a close-up view in the orthorectified image pair generated in ISIS 3 using the temperature-dependent SPICE kernels. It can be seen that the offsets have been largely reduced. However, small offsets can still be noticed. Figure 3 (d) is the close-up view in the orthorectified image pair generated after boresight calibration. It can be seen that the orthorectified NACL image is well aligned with the NACR image, which proves the effectiveness of the boresight calibration approach.

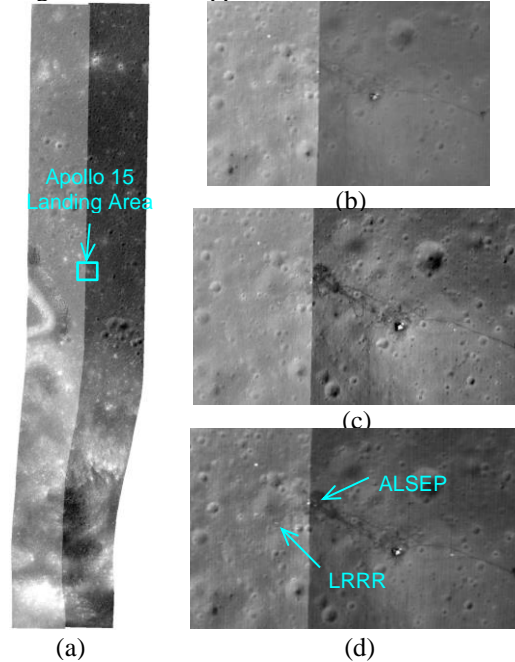


**Figure 3:** Comparison of orthorectified NACL and NACR image pair. (a) Orthorectified image pair showing the Apollo 15 landing area, (b) a close-up view in the orthorectified image pair generated using the standard SPICE kernels, (c) using the temperature-dependent kernels, and (d) after boresight calibration.

**Conclusion:** Considerable changes in the relative boresight alignment between the two NAC cameras do indeed exist. The temperature-dependent SPICE kernels are able to reduce the possible errors in the boresight parameters. However, internal inconsistencies of about 5 - 10 m still exist in the DEMs generated from them. The proposed boresight calibration approach can effectively calibrate the boresight offsets between the NACL and NACR images. This investigation also provides a useful check on the performance of the temperature-dependent SPICE kernels of NAC imagery.

**References:** [1]. Speyerer, E.J. et al. (2014) *Space Science Reviews*. [2]. Robinson, M.S. et al. (2010) *Space Science Reviews*, 150, 81-124. [3]. Wu, B. et al. (2014) *EPSL*, 391, 1-15.